

1 Submarine moraines in Southeast Greenland fjords reveal contrasting outlet-
2 glacier behaviour since the Last Glacial Maximum

3

4 Batchelor, C.L. ^{*1,2}, Dowdeswell, J.A. ², Rignot, E. ^{3,4}, Millan, R. ³

5

6 ¹Norwegian University of Science and Technology (NTNU), NO-7491 Trondheim, Norway

7

8 ²Scott Polar Research Institute, University of Cambridge, Cambridge CB2 1ER, UK;

9 ³Department of Earth System Science, University of California, Irvine, CA, USA;

10 ⁴Jet Propulsion Laboratory, California Institute of Technology, Pasadena, CA, USA;

11

12 * Corresponding author: Christine Batchelor (clb70@cam.ac.uk)

13

14 **Key Points:**

- 15 • We use bathymetric data to identify major moraine ridges in Southeast Greenland
16 fjords
- 17 • Inner-fjord moraines, which were probably formed during the Neoglacial, are
18 widespread along the Southeast Greenland margin
- 19 • Mid-fjord moraines are present beyond the Julianehåb Ice Cap yet are generally
20 absent from the Southeast Greenland Ice Sheet margin

21

22

23

24

25

26 **Abstract**

27 Knowledge of the past behaviour of the outlet glaciers of Southeast (SE) Greenland is
28 necessary to understand and model spatial differences in the response of the Greenland Ice
29 Sheet (GIS) to climatic changes. Here, we use bathymetric data to map the distribution of
30 more than 50 major moraines in SE Greenland fjords. Inner-fjord moraines are widespread
31 along the SE Greenland margin, occurring in 65% of the surveyed fjords. We identify, for the
32 first time, 9 mid-fjord moraines that span the *c.* 150 km long eastern margin of the Julianehåb
33 Ice Cap (JIC). In contrast, mid-fjord moraines are generally absent from the deeper and wider
34 fjords of the SE GIS. The variable distribution of mid-fjord moraines along the SE Greenland
35 margin reveals contrasting behaviour of the SE GIS and the eastern JIC during the last
36 deglaciation, which probably reflects differences in fjord geometry and exposure to ocean
37 heat.

38

39 **1. Introduction**

40 The Southeast (SE) Greenland margin, which includes the SE sector of the Greenland
41 Ice Sheet (GIS) and the eastern Julianehåb Ice Cap (JIC), is drained by a number of fast-
42 flowing, marine-terminating outlet glaciers (Fig. 1). Mountainous terrain and a lack of ice-
43 free areas have largely prevented analysis of the deglacial and Holocene behaviour of these
44 outlet glaciers, although several studies have investigated the past dynamics of the land-
45 terminating outlet glaciers of Southwest (SW) Greenland (Fig. 1c) (Weidick et al., 2004;
46 Winsor et al., 2014; Larsen et al., 2011). The SE Greenland margin is suggested to have been
47 highly sensitive to past climatic changes as a result of its relatively high mass turnover and
48 proximity to major ocean currents, including the Irminger Current, and sites of deep-water
49 formation (Fig. 1a) (Weidick et al., 2004). The fjords of SE Greenland are therefore an ideal
50 location to examine how the climatic changes of the late Quaternary (e.g. Alley et al., 1997)

51 were translated into ice-margin responses. In particular, it is important to identify spatial
52 variations in the past behaviour of Greenland's outlet glaciers, and to understand their
53 controls, to predict the sensitivity or resilience of these outlet glaciers and their future
54 behaviour.

55 Here, we examine bathymetric data from 36 fjords along the *c.*1200 km long SE
56 Greenland margin to reveal the distribution of major submarine moraines (Fig. 1 and Figs. S1
57 to S3 in the supporting information). The geomorphology of these moraines is described
58 alongside their implications for the behaviour of the SE GIS and the eastern JIC since the
59 Last Glacial Maximum (LGM).

60

61 **2. Background: Glacial history**

62 The GIS extended to the shelf break beyond SE Greenland during the LGM (Funder
63 et al., 2004; Roberts et al., 2008; Dowdeswell et al., 2010). Deglacial retreat was underway
64 by around 17 ka (Jennings et al., 2006), driven, in part, by the incursion of warm ($>5^{\circ}\text{C}$),
65 salty, subsurface (> 300 m) water from the Irminger Current (Fig. 1a) (Knutz et al., 2011;
66 Dyke et al., 2014). Our present understanding of the Holocene glacial history of SE
67 Greenland is derived from deglacial ages from major fjords and from studies of threshold
68 lakes and terrestrial moraines in the ice-free zone beyond the Qassimiut Lobe (Fig. 1). The
69 deglacial ice margin is interpreted to have been at the outer coast of SE Greenland by around
70 11 to 10 ka (Bennike and Björck, 2002; Knutz et al., 2011), and to have been retracted behind
71 its present-day extent by around 9 ka for the low-lying Qassimiut Lobe and by about 7 ka in
72 more mountainous regions of SW Greenland (Larsen et al., 2011). In southern Greenland, the
73 maximum Neoglacial (since *c.*4 ka; Anderson et al., 1999) ice extent was generally attained
74 during the Little Ice Age (LIA) of between AD 1450 and 1850, which is marked by a series
75 of terrestrial moraines (Weidick et al., 2004).

76

77 **3. Data and methods**

78 The bathymetric data (Fig. 1) were acquired by NASA's Earth Venture Sub-orbital
79 Oceans Melting Greenland (OMG) mission (OMG mission, 2016). The survey was
80 performed using a Teledyne Reson SeaBat 7160 Multibeam Echo Sounder with a system
81 frequency of 44 kHz and 512 beams. The data were acquired in 2016 using QINSy software
82 and processed using CARIS HIPS software by Terrasond Ltd into a 25-m spacing gridded
83 product. Airborne gravity data are used to show the depth of the seafloor in some inner-fjord
84 areas where bathymetric data are lacking (Fig. 2 and Figs. S1 to S3 in the supporting
85 information), however at a degraded spatial resolution of 750 m. The gravity data were
86 acquired in summer 2016 from an AS350-B3 helicopter using a Sanders Geophysics
87 Airborne Inertially Referenced Gravimeter. Details of gravity data acquisition, processing
88 and inversion modelling are described in Millan et al. (2018). The potential temperature of
89 the water in the fjords (Fig. 2) was sampled at a rate of 16 Hz using two conductivity-
90 temperature-depth (CTD) sensors: an AML Oceanographic Minos X CTD in thick brash/ sea
91 ice and a Valeport Rapid CTD in ice-free conditions (OMG mission, 2016). In this study, the
92 fjords of SE Greenland are labelled 'A' to 'W', from south to north (Figs. 1 and 2 and Figs.
93 S1 to S3 in the supporting information).

94

95 **4. Results**

96 4.1 Broad-scale bathymetry

97 The fjords of SE Greenland are U-shaped in cross-profile and between 20 and 100 km
98 long (Fig. 1). With typical widths of 2 to 3 km, the fjords of the eastern JIC are narrower than
99 those of the SE GIS, which are up to 15 km wide. Fjord water depth beyond the present-day
100 ice margin ranges from 100 to 700 m, with considerable variation between neighbouring

101 fjords (Millan et al., 2018). Although the maximum fjord water depth is similar along the SE
102 Greenland margin, the fjords of the eastern JIC generally have shallower mid-fjord regions
103 (typically 200 to 300 m) compared with those of the SE GIS (typically 400 to 800 m) (Fig. 2
104 and Figs. S1 to S3 in the supporting information). The fjords contain over-deepened basins
105 that are separated by shallower sills. Sills are also present where tributary fjords join the main
106 fjord trunk, yet are generally absent from the innermost region of the fjords (Fig. 2 and Figs.
107 S1 to S3 in the supporting information). The contrasting widths and depths of the fjords along
108 the SE Greenland margin are related to the drainage-basin area of the outlet glaciers that
109 drain into the fjords. The larger outlet glaciers of the SE GIS transferred greater volumes of
110 ice and sediment during periods of ice-sheet advance compared with the smaller outlet
111 glaciers of the JIC, resulting in higher rates of erosion within these fjords.

112 More than 50 large (>10 m high) ridges are identified transverse to the former ice-
113 flow direction in the fjords of SE Greenland (Figs. 2 and 3 and S1 to S3 in the supporting
114 information). These ridges are interpreted as major moraines that record the former positions
115 of still-stands or readvances of the grounding zone.

116

117 4.2 Inner-fjords

118 Major moraine ridges are present in an inner-fjord (landwards third of the fjord
119 length) setting for 26 (*c.*65%) of the fjords of SE Greenland (Fig. 1). The moraines occur
120 between 1.6 and 16 km offshore of the present-day ice margin in water depths of 200 to 550
121 m (Figs. 2 and 3 and Figs. S1 to S3 in the supporting information). The moraines typically
122 have a single crest and are asymmetric with a steeper ice-distal side (Fig. 3c and e). They are
123 up to 2 km long in the former ice-flow direction, up to 150 m above the surrounding seafloor,
124 and span the entire fjord width. Although most inner-fjords are characterised by a single
125 moraine ridge, some contain a sequence of two or three back-stepping features (Fig. 3a;

126 inner-fjord recessional moraines in Fig. 2 and Figs. S1 to S3 in the supporting information).
127 The most seaward moraine in each inner-fjord is located beyond the oldest ice-margin
128 position that has been mapped from aerial photographs obtained in the 1930s (Figs. 2 and 3;
129 Bjørk et al., 2012). Some of the submarine inner-fjord moraines are correlated with
130 prominent terrestrial moraines (Fig. 3a).

131 The submarine ridge beyond Kangerdlussuaq Glacier, which corresponds with the
132 LIA extent of Kjeldsen et al. (2015) as interpreted from terrestrial moraines and trimline
133 heights, has different geometry compared to the other inner-fjord moraines. It comprises
134 high-amplitude ridges at its lateral margins yet has a lower-amplitude wedge-like geometry in
135 its central part (Fig. 3b). It is possible that this feature is an intermediate form between a
136 moraine and a grounding-zone wedge (GZW; Batchelor and Dowdeswell, 2015) that formed
137 when the glacier was grounded at its lateral margins yet had a floating ice shelf over the
138 central, deepest part of the fjord. Short floating sections have been inferred at
139 Kangerdlussuaq Glacier and in other glaciers around Greenland (Joughin et al., 2008).

140

141 4.3 Mid- and outer-fjords

142 Major moraine ridges are present in a mid-fjord setting (close to the fjord mid-point,
143 beyond the inner-fjord moraines) in all of the 9 fjords of the eastern JIC yet in only 1 of the
144 fjords of the SE GIS (Fig. 1b and c). The mid-fjord moraines are located between 8 and 37
145 km from the present-day ice margin in water depths of 200 to 700 m (Figs. 2 and 3). They are
146 up to 3 km long in the former ice-flow direction, reach up to 150 m above the surrounding
147 seafloor, and span the width of the fjord (Fig. 3d and f). Three of the moraines have a double
148 ridge crest, with the crests spaced about 1 km apart (Fig. 3f). Although they occur in a
149 remarkably similar, mid-fjord, position in each of the fjords of the eastern JIC (Fig. 2 and Fig.

150 S3 in the supporting information), the mountainous topography of this area prevents the
151 moraines from being correlated between the fjords.

152 Only one moraine ridge is observed in an outer-fjord setting on the SE Greenland
153 margin. This moraine, which is close to the present-day coastline beyond Anorituup
154 Kangerlua Glacier (Fig. 1c), is around 2 km long and up to 100 m high.

155

156 **5. Discussion**

157

158 5.1 The geomorphological record of past ice dynamics on the SE Greenland margin

159 Our bathymetric data show that the mid- and outer-fjords of the SE GIS and the
160 eastern JIC contain a contrasting geomorphological record of past ice dynamics. Most of the
161 mid- and outer-fjords of the SE GIS for which we have bathymetric data lack
162 geomorphological evidence for major still-stands or readvances of the grounding zone during
163 the last deglaciation (Fig. 1b). This finding is in agreement with other studies that have
164 inferred relatively rapid and continuous deglaciation of the fjords of the SE GIS, which was
165 not punctuated by significant (at least decades to centuries) still-stands or readvances of the
166 ice margin (Roberts et al., 2008; Dyke et al., 2014). In contrast, the presence of large (up to 3
167 km long and 150 m tall) mid-fjord moraines in the fjords of the eastern JIC (e.g. Fig. 3d and
168 f) suggests that the outlet glaciers which occupied these fjords underwent at least one major
169 still-stand or readvance in their grounding-zone position during the last deglaciation.

170 This contrasting style of deglaciation between the SE GIS and the eastern JIC may be
171 a consequence of climatic differences along the SE Greenland margin, for example warmer
172 air and ocean temperatures and/or higher snowfall in the southern part of the margin. The JIC
173 may also have been more sensitive to climatic and oceanographic changes as a result of its
174 proximity to the Irminger Current (Fig. 1a). However, the geometry of the fjords is also

175 important. Whereas relatively rapid ice retreat through the fjords of SE Greenland was
176 encouraged by the considerable depth (up to 1000 m) and width (typically >5 km) of these
177 fjords (Roberts et al., 2008; Dyke et al., 2014), grounding-zone stabilisation would have been
178 encouraged in the mid-fjords of the eastern JIC as a result of their generally shallower and
179 narrower geometry (Figs. 1 and 2 and Figs. S1 to S3 in the supporting information). Narrower
180 and shallower fjords encourage ice-margin stabilisation through increasing basal and lateral
181 drag, which reduces mass flow across the grounding zone, and reducing the rate of iceberg
182 calving, as well as by preventing the incursion of warm subsurface water of Atlantic origin,
183 typically below 300 m depth, to the ice margin (Rignot et al., 2012, 2016; Porter et al., 2014).
184 Our temperature plots show that, at present, the shallower fjords of the eastern JIC block the
185 migration of warm subsurface water of the Irminger Current from reaching a mid- to inner-
186 fjord position (Fig. 2). In contrast, the deep (up to 1000 m) cross-shelf troughs and mid-fjord
187 basins of SE Greenland (Fig. 2 and Figs. S1 to S3 in the supporting information) enable
188 changes in ocean temperature off the shelf to be transmitted more readily through the fjords
189 to the ice margin, encouraging more rapid ice retreat (Millan et al., 2018). The distribution of
190 mid-fjord moraines, as shown in this study (Fig. 1b and c), suggests that this pattern may
191 have also existed along the SE Greenland margin during the last deglaciation.

192 A similar pattern of non-uniform ice-sheet retreat following the LGM, in which the
193 deepest parts of fjords and the continental shelf generally experienced a rapid to episodic
194 style of grounding-zone retreat, has been inferred for other sectors of the GIS (Porter et al.,
195 2014; Batchelor et al., 2018) and on other high-latitude margins (Ó Cofaigh et al., 2008;
196 Stokes et al., 2014). The extent to which warm sub-surface water was able to access the ice
197 margin through deep fjords and cross-shelf troughs has been suggested to have been an
198 important factor in determining the speed and style of deglaciation (Straneo et al., 2010;
199 Dyke et al., 2014). Knowledge of the past behaviour of the SE GIS and JIC is necessary to

200 understand and predict the future dynamics of Greenland's outlet glaciers. The depth and
201 gradient of the seafloor, together with subglacial topography, play an important role in
202 determining the variable ice-marginal response of individual outlet glaciers to atmospheric
203 and oceanographic forcing (Straneo et al., 2010; Rignot et al., 2012; Millan et al., 2018).

204

205 5.2 Chronological implications

206 The most seaward inner-fjord moraine in each fjord is located beyond the oldest ice-
207 margin position known from aerial photographs (Figs. 2 and 3 and Figs. S1 to S3 in the
208 supporting information; Bjørk et al., 2012). Together with their correlation with prominent
209 terrestrial moraines (Fig. 3b; Kjeldsen et al., 2015), this suggests that the inner-fjord moraines
210 were formed sometime during the Neoglacial (since *c.*4 ka). The widespread distribution of
211 the inner-fjord moraines demonstrates that much of the SE sector of the GIS, including the
212 JIC, experienced at least one significant ice-margin still-stand or readvance during this
213 interval, which includes the LIA (AD 1450-1850). However, the outlet glaciers of SE
214 Greenland did not undergo uniform glacier-terminus advance during this time (Fig. 2 and
215 Figs. S1 to S3 in the supporting information). Variations in the magnitude of glacier-terminus
216 advance to/ retreat from the inner-fjord moraines were probably linked with the water depth
217 close to the ice margin and the height of the sub-ice topography, with greater terminus retreat
218 encouraged by deeper fjords with reverse-gradient seafloor slopes (Millan et al., 2018).

219 The broad distribution of the mid-fjord moraines, which spans the *c.*150 km long
220 eastern margin of the JIC (Fig. 1c), together with their similar dimensions, morphology and
221 position within neighbouring fjords (Figs. 2 and 3 and Fig. S3 in the supporting information),
222 suggests that they were formed relatively synchronously. It is unlikely that the relatively
223 small outlet glaciers of the JIC experienced ice-margin readvances during the Neoglacial that
224 were considerably greater than those of the outlet glaciers of the GIS, including the much

225 larger Kangerlussuaq Glacier (16 km; Fig. 3b), which would have experienced higher ice
226 fluxes. It is possible that the mid-fjord moraines were formed during the Younger Dryas (11.6
227 to 12.8 ka), although we note that ice in SE Greenland is generally considered to have been at
228 an inner-shelf to coastline position during this time (Fig. 1; Bennike and Björck, 2002;
229 Jennings et al., 2006; Roberts et al., 2008). Given the distribution of published deglacial ages,
230 which suggest that the ice margin was at the outer coast of SE Greenland by around 11 to 10
231 ka (Bennike and Björck, 2002; Knutz et al., 2011) and retracted behind its present-day extent
232 by around 9 to 7 ka (Larsen et al., 2011; Fig. 1b and c), we hypothesise that the mid-fjord
233 moraines were formed during an ice-margin still-stand or advance that occurred during the
234 early Holocene. It is possible that this still-stand or advance had a climatic control, for
235 example the 8.2 ka event that has been recorded from Greenland ice cores including the Dye-
236 3 site in SE Greenland (Fig. 1b) (Alley et al., 1997). The general absence of mid-fjord
237 moraines from the fjords of the SE GIS is probably related to the greater depth of these
238 fjords, which discouraged ice-margin stabilisation during the early Holocene by enabling the
239 incursion of warm Irminger Current water (Fig. 1a) to the ice margin.

240

241 **6. Conclusions**

242 We use bathymetric data to map, for the first time, major moraine ridges in the fjords
243 of SE Greenland (Fig. 1). Many (*c.*65%) of the inner-fjords of the SE GIS and the eastern JIC
244 contain moraines, which are up to 2 km wide and 150 m tall (Fig. 2 and Figs. S1 to S3 in the
245 supporting information). Their locations beyond the oldest ice-margin position where it is
246 known from aerial photographs and correlation with prominent terrestrial moraines suggest
247 that the inner-fjord moraines were produced sometime during the Neoglacial (since *c.*4 ka).
248 We also identify a series of 9 major (up to 3 km long and 150 m tall) mid-fjord moraines in
249 the fjords of the eastern JIC (Figs. 1c, 3c to f). In contrast, mid-fjord moraines are generally

250 absent from the deeper and wider fjords of the SE GIS to the north, in which relatively rapid
251 and continuous ice retreat is interpreted to have occurred during the last deglaciation. We
252 hypothesise that the mid-fjord moraines of the eastern JIC were formed during an ice-cap-
253 wide still-stand or readvance that was superimposed upon regional deglaciation following the
254 LGM. Contrasting behaviour between the SE GIS and the JIC since the LGM is interpreted to
255 be a consequence of the shallower and narrower fjord geometry of the JIC, which encouraged
256 ice-margin stabilisation by reducing the rate of iceberg calving and stronger modulation of
257 the incursion of warm subsurface water to the glacier termini by prevailing currents and
258 winds. Our submarine mapping work provides further incentive to understand, and provide
259 chronological control on, the past behaviour of the marine-terminating outlet glaciers of this
260 region of the GIS.

261

262 **7. Acknowledgments and Data**

263 There are no conflicts of interest for any author. Profiles through all surveyed fjords
264 are shown in Figs. S1 to S3 in the supporting information. We thank NASA's Oceans Melting
265 Greenland (OMG) project and the crew of the M/V Neptune for collecting the bathymetric
266 and water temperature data in SE Greenland. The data are contained at:

267 <http://dx.doi.org/10.5067/OMGEV-BTYSS>, at <http://omg.jpl.nasa.gov>, and at

268 <https://faculty.sites.uci.edu/erignot/>. During this work, C.L. Batchelor was in receipt of a

269 Junior Research Fellowship at Newnham College, University of Cambridge, and a VISTA

270 scholarship to the Norwegian University of Science and Technology (NTNU), Trondheim,

271 Norway. We wish to thank two anonymous reviewers for their helpful reviews of this paper.

272

273 **8. References**

274 Anderson, N. J., Bennike, O., Christoffersen, K., Jeppesen, E., Markager, S., Miller,
275 G., & Renberg, I. (1999). Limnological and palaeolimnological studies of lakes in south-
276 western Greenland. *Geology of Greenland Survey Bulletin*, 183, 68-74.

277 Alley, B. B., Mayewski, P. A., Sowers, T., Stuiver, M., Taylor, K. C., & Clark, P. U.
278 (1997). Holocene climatic instability: A prominent, widespread event 8200 yr ago. *Geology*,
279 25, 483-486.

280 Batchelor, C. L., & Dowdeswell, J. A. (2015). Ice-sheet grounding-zone wedges
281 (GZWs) on high-latitude continental margins. *Marine Geology*, 363, 65-92.

282 Batchelor, C. L., Dowdeswell, J. A., & Rignot, E. (2018). Submarine landforms
283 reveal varying rates and styles of deglaciation in North-West Greenland fjords. *Marine*
284 *Geology*, 402, 60-80.

285 Bennike, O., & Björck, S. (2002). Chronology of the last recession of the Greenland
286 Ice Sheet. *Journal of Quaternary Science*, 17, 211-219.

287 Björk, A. A., Kjær, K. H., Korsgaard, N. J., Khan, S. A., Kjeldsen, K. K., Andresen,
288 C. S., et al. (2012). An aerial view of 80 years of climate-related glacier fluctuations in
289 southeast Greenland. *Nature Geoscience*, 5, 427-432.

290 Dowdeswell, J. A., Evans, J., & Ó Cofaigh, C. (2010). Submarine landforms and
291 shallow acoustic stratigraphy of a 400 km-long fjord-shelf-slope transect, Kangerlussuaq
292 margin, East Greenland. *Quaternary Science Reviews*, 29, 3359-3369.

293 Dyke, L. M., Hughes, A. L. C., Murray, T., Hiemstra, J. F., Andresen, C. S., & Rodés,
294 A. (2014). Evidence for the asynchronous retreat of large outlet glaciers in southeast
295 Greenland at the end of the last glaciation. *Quaternary Science Reviews*, 99, 244-259.

296 Funder, S., Jennings, A., & Kelly, M. (2004). Middle and late Quaternary glacial
297 limits in Greenland. *Developments in Quaternary Sciences*, 2, 425-430.

298 Jakobsson, M., Mayer, L., Coakley, B., Dowdeswell, J. A., Forbes, S., Fridman, B., et
299 al. (2012). The International Bathymetric Chart of the Arctic Ocean (IBCAO) Version 3.0.
300 *Geophysical Research Letters*, 39, L12609.

301 Jennings, A. E., Hald, M., Smith, M., & Andrews, J. T. (2006). Freshwater forcing
302 from the Greenland Ice Sheet during the Younger Dryas: evidence from southeastern
303 Greenland shelf cores. *Quaternary Science Reviews*, 25, 282-298.

304 Joughin, I., Howat, I., Alley, R. B., Ekström, G., Fahnestock, M., Moon, T., Nettles,
305 M., Truffer, M., & Tsai, V. C. (2008). Ice-front variations and tidewater behaviour on
306 Helheim and Kangerdlugssuaq Glaciers, Greenland. *Journal of Geophysical Research*, 113,
307 F01004.

308 Joughin, I., Smith, B., Howat, I., & Scambos, T. (2010). MEaSURES Greenland Ice
309 Velocity Map from InSAR Data. NASA DAAC at the National Snow and Ice Data Center,
310 Boulder, Colorado, USA. [http://dx.doi.org/10.5067/MEASURES/CRYOSPHERE/nsidc-](http://dx.doi.org/10.5067/MEASURES/CRYOSPHERE/nsidc-0478.001)
311 0478.001.

312 Kjeldsen, K. K., Korsgaard, N. J., Bjørk, A. A., Khan, S. A., Box, J. E., Funder, S., et
313 al. (2015). Spatial and temporal distribution of mass loss from the Greenland Ice Sheet since
314 AD 1900. *Nature*, 528, 396-400.

315 Knutz, P. C., Sicre, M-A., Ebbesen, H., Christiansen, S., & Kuijpers, A. (2011).
316 Multiple-stage deglacial retreat of the southern Greenland Ice Sheet linked with Irminger
317 Current warm water transport. *Paleoceanography and Paleoclimatology*, 26, PA3204.

318 Korsgaard, N. J., Nuth, C., Khan, S. A., Kjeldsen, K. K., Bjørk, A. A., Schomacker,
319 A., & Kjær, K. H. (2016). Digital elevation model and orthophotographs of Greenland based
320 on aerial photographs from 1978-1987. *Scientific data*, 3, 160032.

321 Larsen, N. K., Kjær, K. H., Olsen, J., Funder, S., Kjeldsen, K. K., & Nørgaard-
322 Pedersen, N. (2011). Restricted impact of Holocene climate variations on the southern
323 Greenland Ice Sheet. *Quaternary Science Reviews*, 30, 3171-3180.

324 Millan, R., Rignot, E., Mouginit, J., Wood, M., Bjørk, A. A., & Morlighem, M.
325 (2018). Vulnerability of southeast Greenland glaciers to warm Atlantic Water from Operation
326 IceBridge and Ocean Melting Greenland data. *Geophysical Research Letters*, 45, 2688-2696.

327 OMG Mission, 2016. Bathymetry (sea floor depth) data from the ship-based
328 bathymetry survey. <http://dx.doi.org/10.5067/OMGEV-BTYSS>, Ver. 0.1, Accessed: October
329 2016.

330 Ó Cofaigh, C., Dowdeswell, J. A., Evans, J., & Larter, R. D. (2008). Geological
331 constraints on Antarctic palaeo-ice stream retreat. *Earth Surface Processes and Landforms*,
332 33, 513-525.

333 Porter, D. F., Tinto, K. J., Boghosian, A., Cochran, J. R., Bell, R. E., Manizade, S. S.,
334 & Sonntag, J. G. (2014). Bathymetric control of tidewater glacier mass loss in northwest
335 Greenland. *Earth and Planetary Science Letters*, 401, 40-46.

336 Rignot, E., Fenty, I., Menemenlis, D., & Xu, Y. (2012). Spreading of warm ocean
337 waters around Greenland as a possible cause for glacier acceleration. *Annals of Glaciology*,
338 53, 257-266.

339 Rignot, E., Xu, Y., Menemenlis, D., Mouginit, J., Scheuchl, B., Li, X., et al. (2016).
340 Modeling of ocean-induced ice melt rates of five west Greenland glaciers over the past two
341 decades. *Geophysical Research Letters*, 43, 6374-6382.

342 Roberts, D. H., Long, A. J., Schnabel, C., Simpson, M., & Freeman, S. (2008). The
343 deglacial history of the southeast sector of the Greenland ice sheet during the Last Glacial
344 maximum. *Quaternary Science Reviews*, 27, 1505–1516.

345 Stokes, C. R., Corner, G. D., Winsborrow, M. C. M., Husum, K., & Andreassen, K.
346 (2014). Asynchronous response of marine-terminating outlet glaciers during deglaciation of
347 the Fennoscandian Ice Sheet. *Geology*, 42, 455-458.

348 Straneo, F., Hamilton, G. S., Sutherland, D. A., Stearns, L. A., Davidson, F.,
349 Hammill, M. O., Stenson, G. B. & Rosing-Asvid, A. (2010). Rapid circulation of warm
350 subtropical waters in a major glacial fjord in East Greenland. *Nature Geoscience*, 3, 182-186.

351 Weidick, A., Kelly, M., & Bennike, O. (2004). Late Quaternary development of the
352 southern sector of the Greenland Ice Sheet, with particular reference to the Qassimiut lobe.
353 *Boreas*, 33, 284-299.

354 Winsor, K., Carlson, A. E., Rood, D. H. (2014). ^{10}Be dating of the Narsarsuaq
355 moraine in southernmost Greenland: evidence for a late-Holocene ice advance exceeding the
356 Little Ice Age maximum. *Quaternary Science Reviews*, 98, 135-143.

357

358 **9. Figure Captions**

359

360 **Figure 1.** The distribution of bathymetric data used in this study. (a) Map of SE Greenland
361 and major ocean currents. BB = Baffin Bay; EC = East Greenland Current; IC = Irminger
362 Current; LS = Labrador Sea; NAO = North Atlantic Ocean; WC = West Greenland Current.

363 (b) Map of the SE Greenland margin, showing OMG bathymetric data and the distribution of
364 submarine moraines. Yellow circles are published ^{10}Be and ^{14}C deglacial ages (Roberts et al.,
365 2008; Dyke et al., 2014). GT = Gyldenløves Trough; KT = Kangerdlussuaq Trough; SKT =
366 Skjoldungen Trough; Background is IBCAO bathymetry (Jakobsson et al., 2012) with 200 m
367 contours and colour coded from black (deep) to white (shallow). The average ice velocity of
368 the GIS (2000 to 2009) is from NASA's Making Earth System Data Records for Use in
369 Research Environments (MEaSUREs) program (Joughin et al., 2010). Dashed red line is

370 boundary between GIS and JIC. (c) Map of the Julianehåb Ice Cap (JIC), showing published
371 ^{10}Be and ^{14}C deglacial ages (Weidick et al., 2004; Bennike and Björck, 2002; Larsen et al.,
372 2011; Winsor et al., 2014). Purple line is Tunugdliarfik moraines (Weidick et al., 2004). AK
373 = Anorituup Kangerlua Glacier. ANT = Anoritup Trough; LT = Lindenow Trough; NT =
374 Napassorsuaq Trough; PT = Patussoq Trough.

375

376 **Figure 2.** Selected profiles along the fjords of SE Greenland, showing the locations of major
377 moraines and the potential water temperature of the fjords. Profiles start at 2016 glacier
378 position. Black and dark grey areas show seafloor depth from OMG bathymetric data and
379 free-air gravity anomaly data, respectively. Dashed red lines are former outlet-glacier
380 positions. Potential water temperature is from conductivity-temperature-depth (CTD) casts,
381 with CTD positions shown by grey lines.

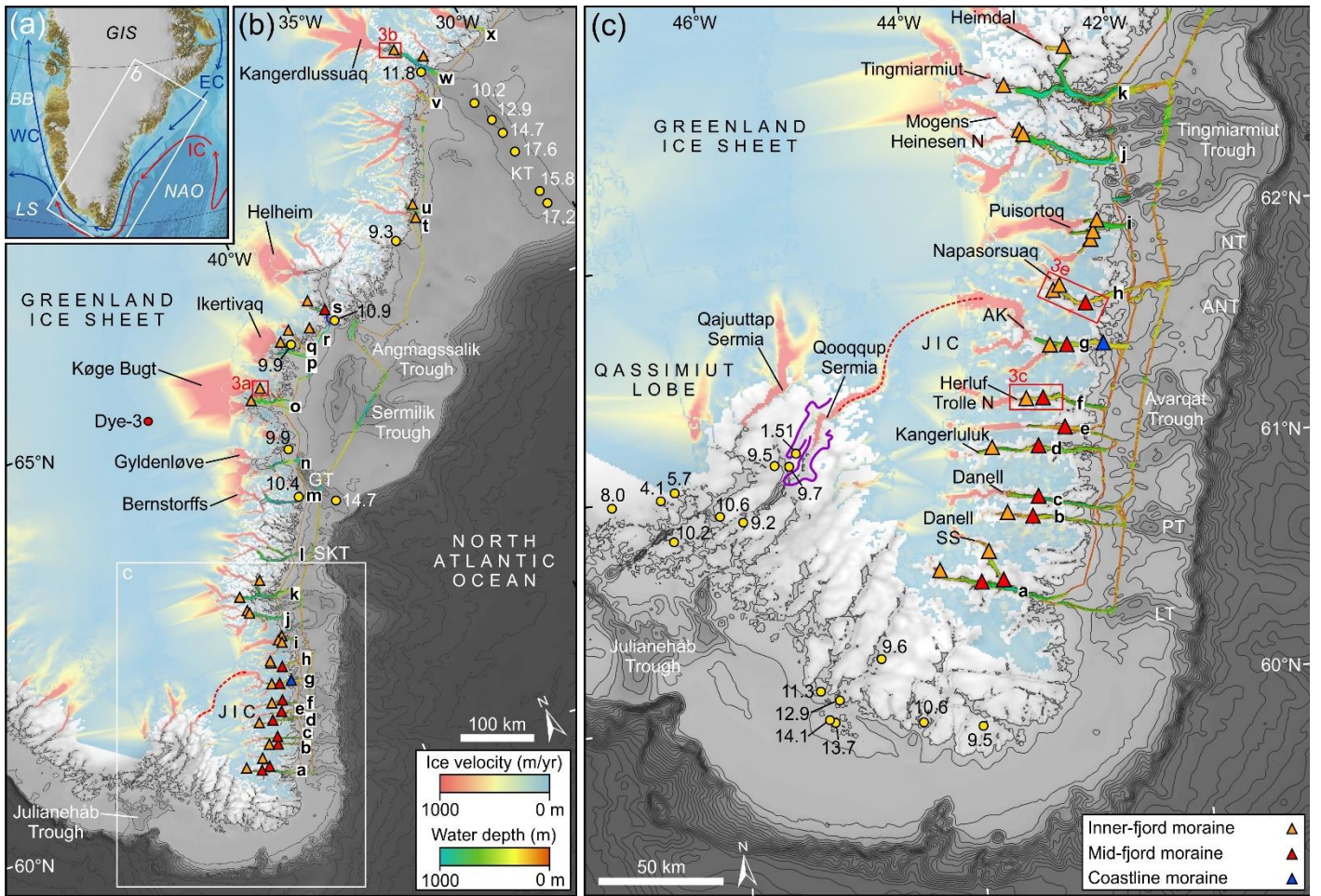
382

383 **Figure 3.** Bathymetric examples of moraines in SE Greenland fjords. Grid cell-size is 25 m.
384 Locations are in Fig. 1. (a) Inner-fjord moraines beyond Køge Bugt North Glacier (Fjord
385 ‘O2’). Background is 1981 aerial photograph from G150 AERODEM dataset (Korsgaard et
386 al., 2016). Red arrows show terrestrial moraines. (b) Inner-fjord ridge/wedge beyond
387 Kangerdlussuaq Glacier (Fjord ‘W1’). Background is Landsat 8 satellite imagery acquired in
388 2016. (c) Bathymetric data beyond Herluf Trolle North Glacier (Fjord ‘F’), showing inner-
389 and mid-fjord moraines. (d) Detail of the mid-fjord moraine in (c). (e) Bathymetric data
390 beyond Napassorsuaq Glacier (Fjord ‘H1’), showing inner- and mid-fjord moraines. (f) Detail
391 of the mid-fjord moraine in (e).

392

393

394



408

409 Figure 1.

410

411

412

413

414

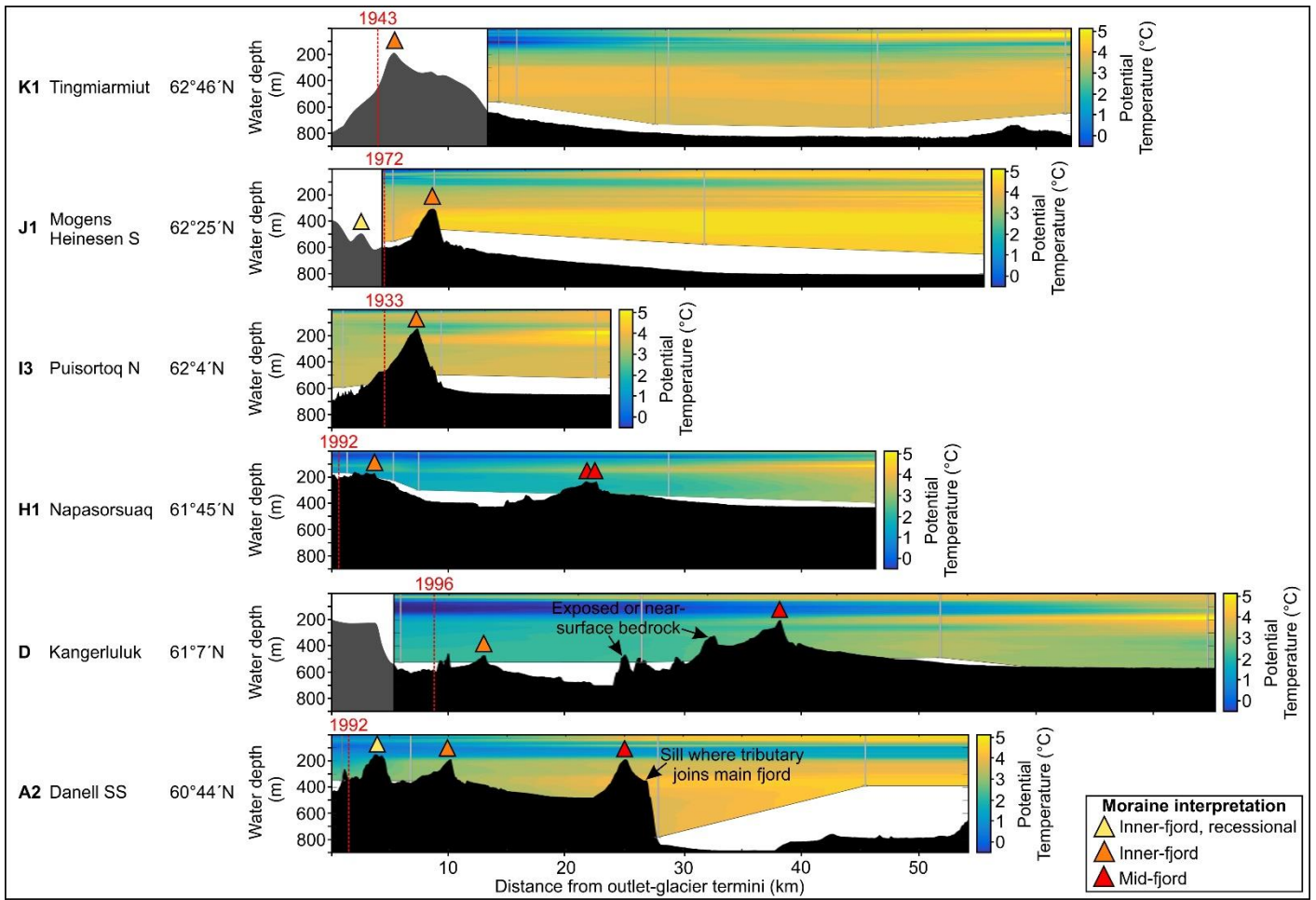
415

416

417

418

419



433 Figure 2.

434

435

436

437

438

439

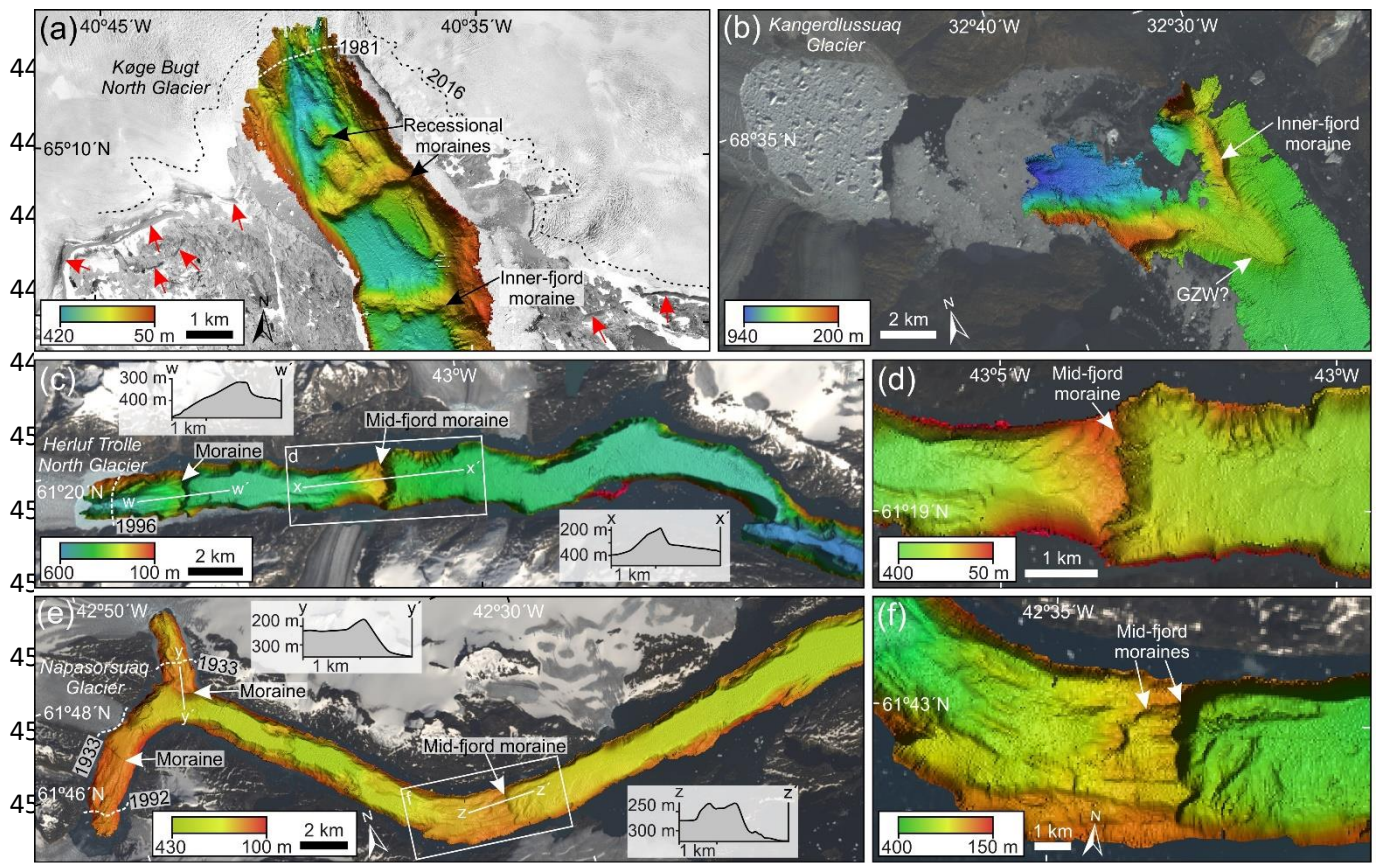
440

441

442

443

444



456

457 Figure 3.

Supporting Information

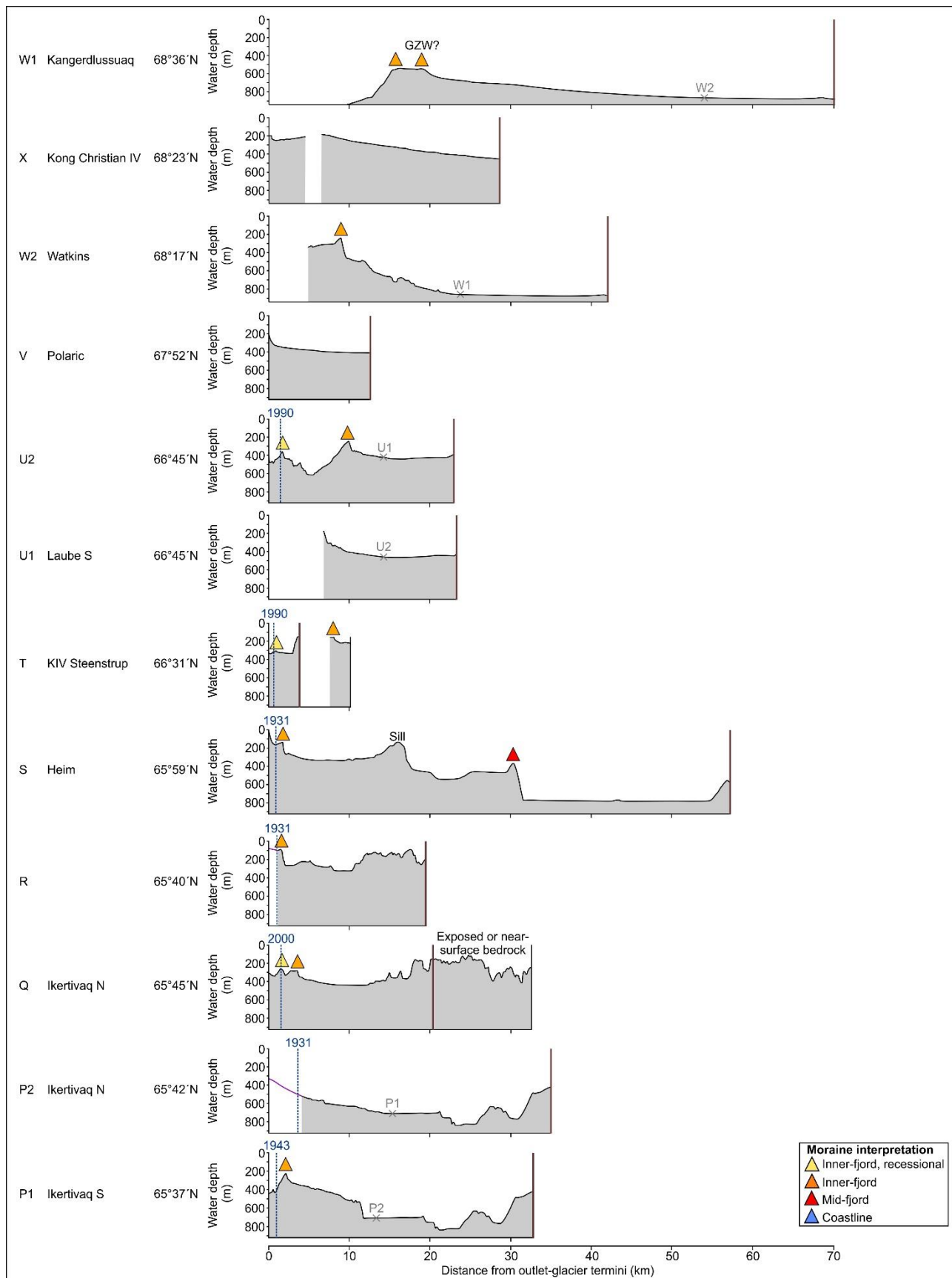


Figure S1. Profiles along the surveyed fjords of SE Greenland, showing the locations of major (> 10 m high) moraines in fjords 'P' to 'W'. With the exception of in Fjords U2 and T, which are short fjords of less than 25 km in length, moraines are classified as 'inner-fjord'

Supporting Information

when they are present within the landward third of the total fjord length. 'Mid-fjord' moraines are defined as those that are close to the mid-point of the length of each fjord. 'Inner-fjord recessional' moraines are those that are landwards of another inner-fjord moraine. Profiles start at 2016 glacier position. Grey areas are seafloor depth from OMG bathymetric data. Purple lines are seafloor depth derived from free-air gravity anomaly data (Millan et al., 2018). Dashed blue lines show the oldest ice-margin position that has been mapped from aerial photographs (Bjørk et al., 2010). Vertical brown lines show the approximate position of the present-day coastline. Fjords are labelled 'A' to 'W' from south to north, as in Fig. 1, with numbers denoting tributaries of the main fjords. Grey crosses show the position at which tributary fjords converge. GZW = Grounding-zone wedge.

Supporting Information

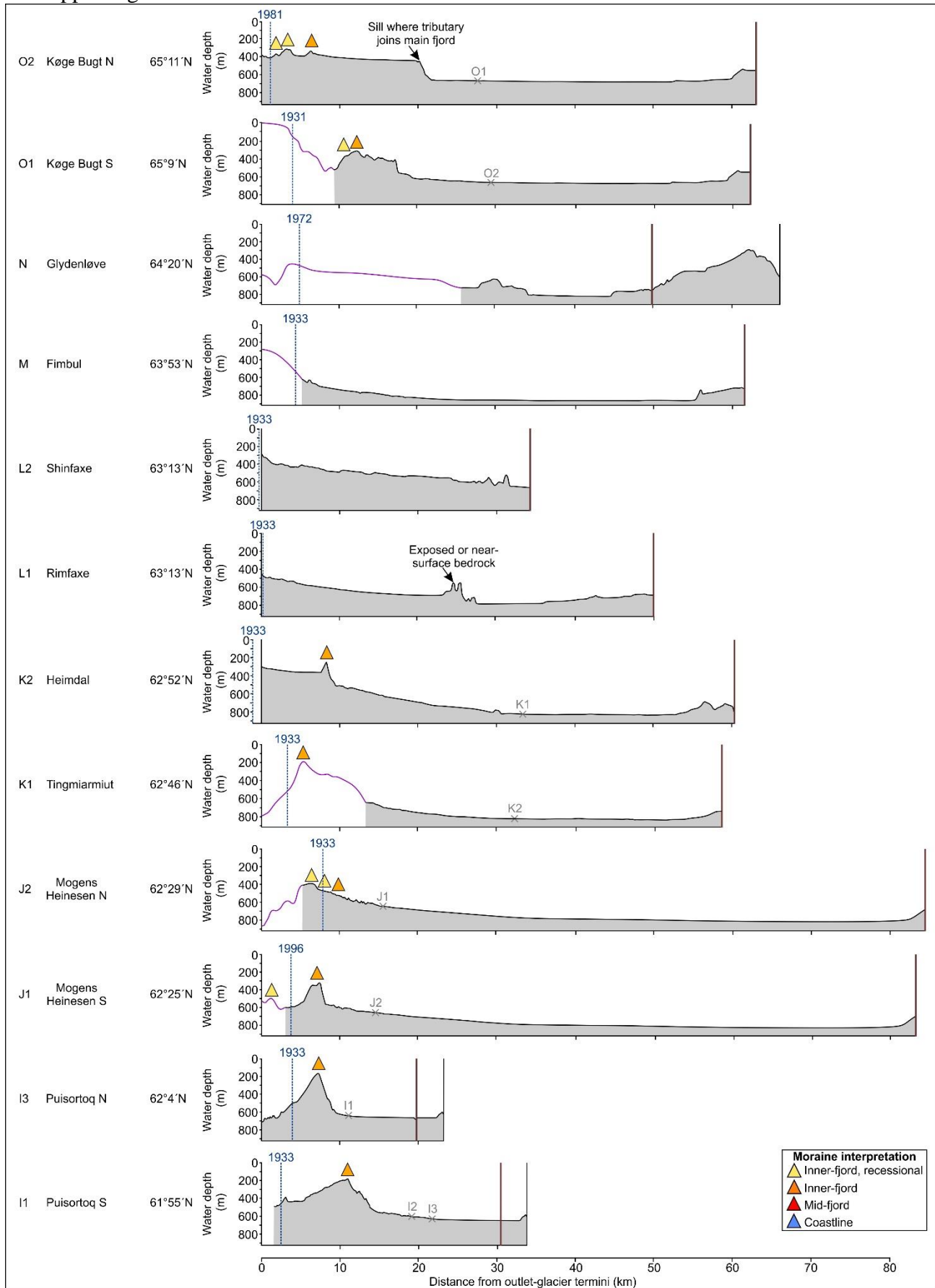
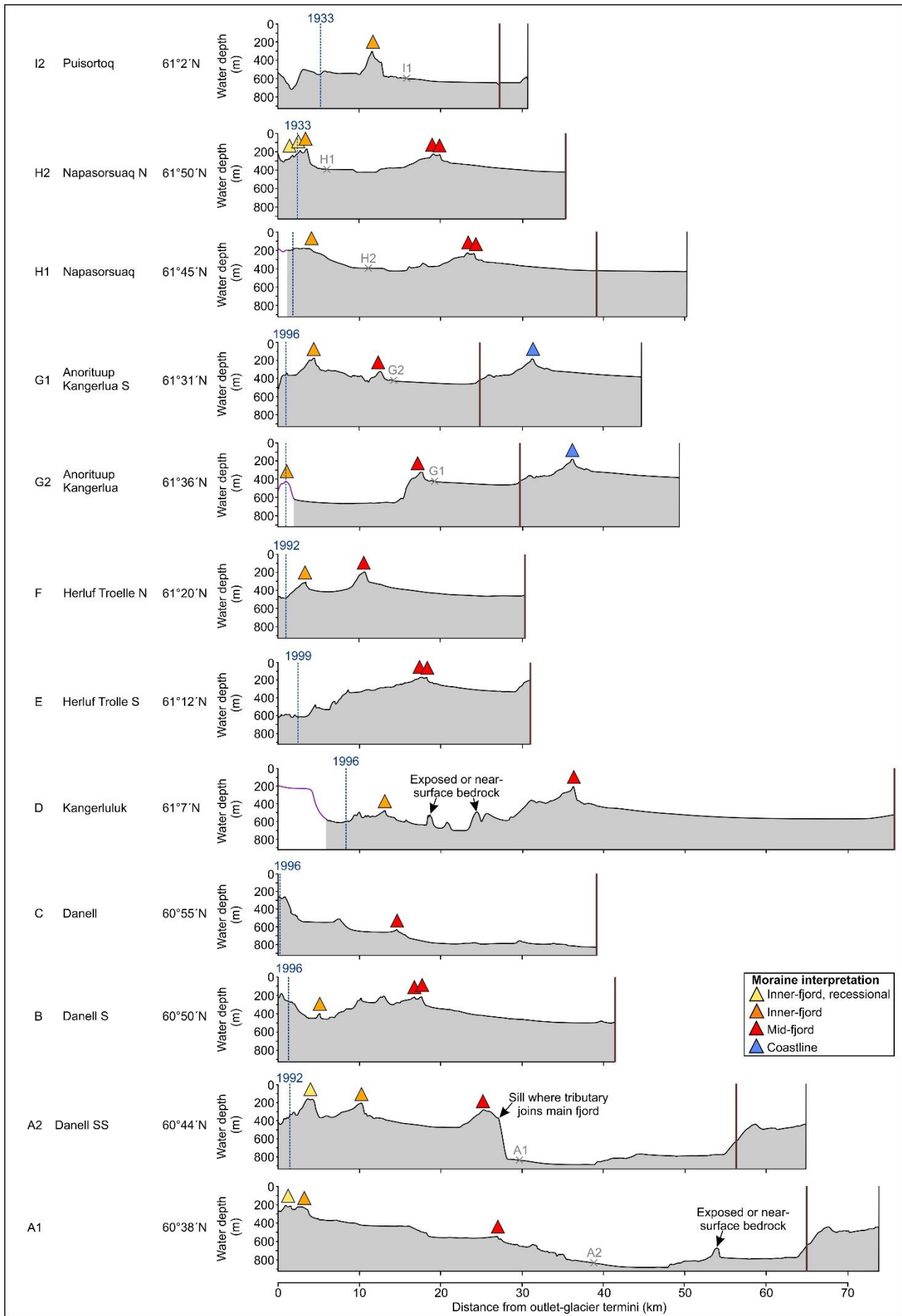


Figure S2. Profiles along the surveyed fjords of SE Greenland, showing the locations of major (>10 m high) moraines in fjords 'O' to 'I'. Key is the same as in Fig. S1.

Supporting Information



Supporting Information

Figure S3. Profiles along the surveyed fjords of SE Greenland, showing the locations of major (>10 m high) moraines in fjords 'I' to 'A'. Key is the same as in Fig. S1.